MSc in Photonics

PHOTONICS**BCN**

Universitat Politècnica de Catalunya (UPC)
Universitat Autònoma de Barcelona (UAB)
Universitat de Barcelona (UB)
Institut de Ciències Fotòniques (ICFO)

http://www.photonicsbcn.eu

Master in Photonics

MASTER THESIS WORK

NARROWBAND PHOTON PAIR SOURCE COMPATIBLE WITH SOLID STATE QUANTUM MEMORIES

Darío Lago Rivera

Supervised by Dr./Prof. Hugues De Riedmatten, (ICFO)
Co-supervised by Dr. Andreas Lenhard (ICFO)

Presented on date 8th September 2016

Registered at

Escola Tècnica Superior d'Enginyeria de Telecomunicació de Barcelona

Narrowband photon pair source compatible with solid state quantum memories

Darío Lago Rivera

ICFO, Institut de Ciències Fotòniques, Mediterranean Technology Park, 08860 Castelldefels (Barcelona), Spain

E-mail: dario.lago@icfo.es

September 2016

Abstract. The generation of narrowband photon pairs compatible with solid state quantum memories is shown and analysed. This study is made in two different steps. In the beginning we implement a photon pair source with a periodically poled lithium niobate crystal in free space configuration. The photon pairs are characterized and their cross-correlation is measured. The source is also used as heralded single photon source, with the single photon character shown with a direct antibunching measurement. In a second step the crystal is embedded in a resonator to generate narrowband photons. Cavity enhancement is observed and the quantum behaviour of the photons is analysed. The final source is able to generate photon pairs with one photon at 606 nm while the other photon, at 1436 nm, will be used as herald. The biphoton bandwidth is <3 MHz making it compatible with a Pr^{3+}:Y_2SiO_5 solid state quantum memory.

Keywords: photon pair source, narrowband single photons, parametric down conversion

1. Introduction

To exchange quantum information over large distances in optical fibres, *quantum repeater networks* are necessary. Such architectures [1] can be implemented with *quantum memories (QM)* connected by entangled pairs of photons (see Fig. 1). In that scheme, one photon of the pair is absorbed in the QM, so it has to be resonant with its transition, while its partner is sent over long distances to an intermediate station where it interacts with a photon from a neighbouring node. To this end it is advantageous to have this second photon at low-loss telecom wavelength. Using *entanglement swapping*, the remote memories can be entangled. The goal of this thesis is to develop a photon pair source compatible with such a scheme.

Solid state QM based on Pr^{3+}:Y_2SiO_5 are good candidates for storing the single photons [2]. This restricts the wavelength of the absorbed photons to 606 nm with a linewidth below 4 MHz due to the limited absorption bandwidth of this material [2]. A compatible source had already been developed before [3, 4] and recently used in our group to store single photons in a Pr^{3+}:Y_2SiO_5 solid state QM [2]. However, in the current version [4], the biphoton linewidth is around 2.8 MHz, too large for a full

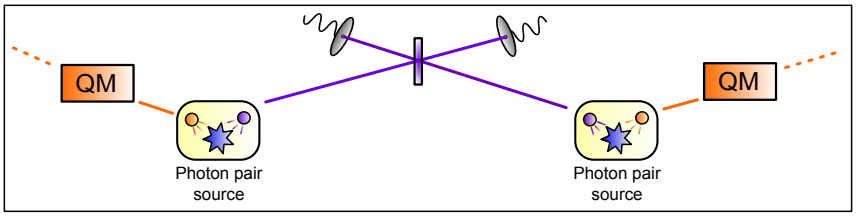

Figure 1. Scheme of two QM connected by entanglement.

absorption in the QM. Here, we report on a new design that outperforms the old one in terms of linewidth. This is achieved by an improved resonator design, which will be discussed in detail.

One resource to generate photon pairs is the second order non linear effect *Spontaneous Parametric Down Conversion (SPDC)*. The interest of this phenomenon for the field of quantum optics keeps increasing since it was demonstrated that it can be a source of entanglement [5]. The basic idea behind this process is the splitting of a pump photon into two photons of lower energy (called signal and idler) within a nonlinear material. The quantum state of the photon pair can be described by [2]: $|\Psi\rangle_{s,i} = \sqrt{1-p}\sum_{n=0}^{\infty} p^{n/2} |n\rangle_s |n\rangle_i$. This state is known as two-mode squeezed state. Here p is the generation probability, which is proportional to the pump power and $|n\rangle_s(|n\rangle_i)$ is the n photon Fock state for the signal (idler) field. It provides strong correlations in creating signal and idler photons.

When an idler photon is detected, there must be a signal photon present due to the correlations. This effect is exploited to generate heralded single photons. The purity of such heralded single photons decreases for high pump powers since the generation of multiple pairs becomes more probable [6].

One drawback of using this effect as resource to obtain single photons is that their spectrum is too broad for QM (of the order of hundreds of GHz). To reduce the linewidth the nonlinear medium is embedded in an optical resonator [7]. The photons can then only be created within the cavity modes resulting in spectral enhancement. The photons can thus be shaped by the cavity design.

This thesis is organised as follows: In section 2 we give a brief introduction of the figures of merit that will be used to characterize the performed experiments. In section 3 we discuss the cavity design. In section 4 we describe a first experiment without embedding the crystal inside a cavity. Eventually, in section 5 we show the generation of narrowband photons pairs in a *cavity enhanced* experiment.

2. Figures of merit

The main parameters that will be used as figure of merit in order to characterise both, the free space and cavity enhanced single photon generation are:

- **Second order normalised cross-correlation ($g^{(2)}_{s,i}(\Delta t)$):** It is defined by $g^{(2)}_{s,i}(\Delta t) = \frac{p_{s,i}}{p_s p_i}$. Here $p_{s,i}$ is the probability to detect a coincidence, while p_s and p_i

are the probabilities for detection of a single signal or idler photons, respectively. This value is commonly used to quantify the quality of the correlation between the signal and the idler. The Cauchy-Schwarz inequality introduces an upper boundary for classical correlations. With the additional assumptions that the signal and idler fields have thermal statistics this implies non-classical correlations for $g^{(2)}_{s,i}(\Delta t) > 2$ [2]. In this work, the value of $g^{(2)}_{s,i}(\Delta t)$ will be calculated by first generating a time-resolved histogram of a signal-idler coincidence measurement. For $p_{s,i}$ all the coincidences around the peak of correlations are integrated (see Fig. 4(b)).

- **Heralded auto-correlation ($g^{(2)}_{i:s,s}$):** This figure will be used to show the single photon behaviour of the signal field. The base is an anti-bunching experiment where the signal is split by a beam splitter but the idler will be used to trigger the measurements. In the end, triple coincidences (between one idler photon and one split signal photon) are measured. The observation of a dip in the histogram means a non classical behaviour. In addition, for an ideal single photon there cannot be coincidences after the beam splitter, hence $g^{(2)}_{i:s,s}$ tends to 0. The $g^{(2)}_{i:s,s}(\Delta t)$ value is found by comparing the height of the central bin with the average of the outer bins in the histogram. For two-mode squeezed state and for low pump powers the heralded auto-correlation is proportional to the inverse of the cross-correlation [4].
- **Coincidences rate:** This value will tell us how many times per second we have a coincidence between a signal and an idler detection.
- **Klyshko efficiency (η_K):** It can be defined as the ratio between the coincidence rate and the single counts detected only looking at the idler (signal). Hence it is the probability to detect a signal (idler) photon after having detected an idler (signal) one [8]. If η_K is corrected by the detection efficiency, we obtain the **Heralding efficiency (η_H)**.

3. Designing the cavity

The basic scheme used consists of a ring cavity as can be seen in the Fig. 2(a). A constrain to the design of the cavity is to use an already existing crystal, which is a copy of the one installed in the existing source [3] as well as using already available mirrors with the same coating of that source. The degrees of freedom in the design to optimise performance are thus different radius of curvature for the mirrors and their relative positions. As these mirrors have the same reflectivity as before, in order to achieve smaller bandwidth, a smaller free spectral range (FSR), i.e. a longer cavity should be designed.

Another degree of freedom for the performance is the focusing of the pump beam to the crystal and the mode matching of the emission to the resonator. The optimal focusing condition for efficient non linear effect is given by $\omega^2 = \lambda d_{crystal}/(2\pi\epsilon_{BK})$ where $\epsilon_{BK} = 2.84$ is the Boyd-Kleinman factor [9].

In addition, I programmed a *Matlab* self-made script where the resonator stability

condition [10], the symmetry of the shape of the waist through the optical path inside the cavity and a fixed angle of incidence and reflexion of 10 degrees were also taken into account. A final comparison was made between all the possible outcomes from the program where, using gaussian optics, the waists through the resonator of the involved frequencies were simulated.

The design that was finally chosen is shown in Fig. 2(a) giving a $FSR = 265$ MHz and its corresponding waist shape is shown at 2(b).

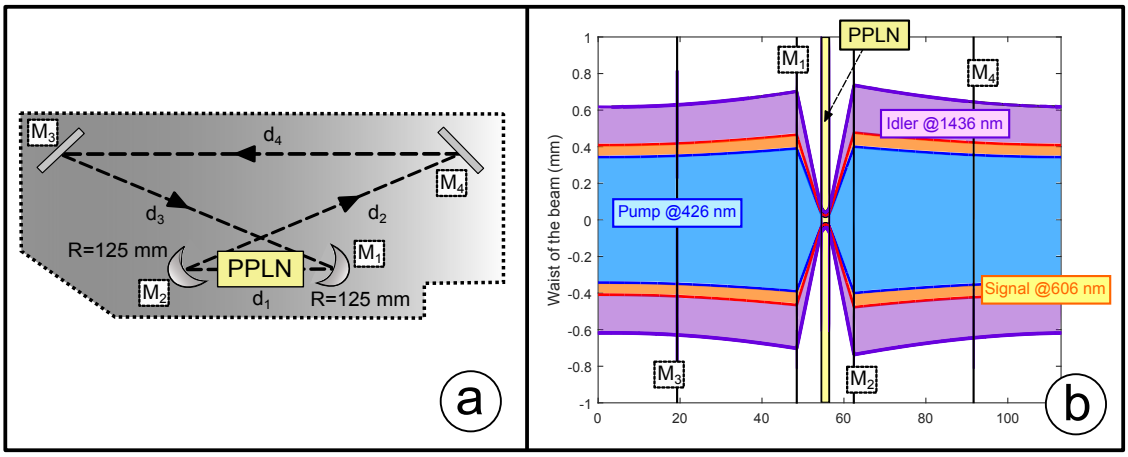

Figure 2. (a) Physical design of the cavity. Ring design centering the PPLN crystal between both spherical mirrors, M_1 and M_2 (both having a radius of curvature of 125 mm). Mirrors M_3 and M_4 are flat mirrors. M_3 is the output mirror with 97% reflectivity. The labelled dimensions are: $d_1 = 139.6mm$, $d_2 = d_3 = 292mm$, $d_4 = 409mm$ and $R = 125mm$ **(b) Design of the beams waists inside the cavity.** The beam shape is designed to be symmetric for all the fields with a waist in the crystal and one between M_3 and M_4.

4. Creating single photons: Free space experiment

In this section the non linear crystal will be characterized without embedding it into a cavity. A 2 cm long lithium niobate crystal is used for the SPDC process. It is designed for type-I phase matching by periodic poling (PPLN) with a poling period of 16.5 μm. Thus signal and idler field have the same polarisation. The pump is a cw beam of 426 nm and the phase matching leads to a signal at 606 nm while the idler is at 1436 nm in the so-called telecom E-band.

Fig. 3(a) shows the experimental setup. The measurements are done in a setup similar to the cavity one except that one mirror has been removed. A dichroic mirror which is reflective in the visible range and transmissive in the infrared is used to split the photons. In order to protect the single photon detectors two main precautions have been taken: **(1)** A great amount of the power of the pump beam is lost behind the crystal since the cavity mirrors have almost no reflexion effect at its wavelength. **(2)** Just before both fibres, dielectric filters suppress residual pump and most of the background light.

In a first set of measurements the coincidences between the signal and the idler were studied, the results are illustrated in Fig. 3 (b) & (c). The detector for the idler photons (Id Quantique Id230 InGaAs avalanche photodiode) has an adjustable dead time. In a first measurement it was set to 25 μs leading to a saturation effect in the detected counts. The saturation could be avoided by decreasing the deadtime to 2 μs leading to higher noise (e.g. afterpulsing). These increased noise effects produce a lower Klyshko efficiency (see Fig. 3 (c) - *right Y axis*). In the unsaturated case a coincidence rate of 2300 $\frac{counts}{s \cdot mW}$ is observed (3 (c) - *left Y axis*).

Focusing now our attention on the cross-correlation curve (using a time-window of $\Delta t = 6ns$), we observe a maximum $g^{(2)}_{s,i}(\Delta t)$ value of $6 \cdot 10^4$ at pump power around 1 μW. When the pump power is further decreased the $g^{(2)}_{s,i}(\Delta t)$ value decreases as the photon count rates become comparable to the dark counts, which are not correlated. On the other hand, the $g^{(2)}_{s,i}(\Delta t)$ value decreases for high pump powers as the generation probability for multiple pairs increases. In the case of 1 mW of pump power we find $g^{(2)}_{s,i}(\Delta t) = 210$.

We also measured the heralded autocorrelation of the signal photon. The explanation of its behaviour is analogous to the cross-correlation case. Indeed we find a proportionality constant of 2.5 between these values and the inverse of the cross-correlation. We reach a minimum value of $1.3 \cdot 10^{-4}$.

The dependence of the cross-correlation and the heralded auto-correlation on power is modelled assuming the probability of generating the pair of photons proportional to this pump power and detector imperfections: dark counts, efficiency and even their jitter [11].

5. Getting narrow photons: Cavity Characterisation

To generate narrow band photons the cavity is now closed by adding a fourth mirror to the previous (free space) setup (Fig. 4(a)). The same measurements as before are performed to compare the characteristics of the narrow band photons with the original ones. A reference beam at 606 nm is coupled to the cavity in order to easily align it with the help of the transmitted light measured on the photodiode (PD1). Also a second photodiode (PD2) is installed to collect the reflected light from the cavity. Because of this, when the cavity is resonant, the reflected reference beam will also be affected, allowing the generation of an error signal useful afterwards for the locking.

Another important difference respect to the previous setup is the piezoelectric ring that is glued to one of the flat mirrors and is used to change the cavity length, which will help in the lock and stability of the cavity. For the measurements shown here the length of the cavity is scanned.

The main experiments performed to characterize the source are the following:

- **Linewidth and free spectral range:** Coincidence histograms (as the ones that can be seen in the Fig. 4 (b)) were used to analyse both, the linewidth and the

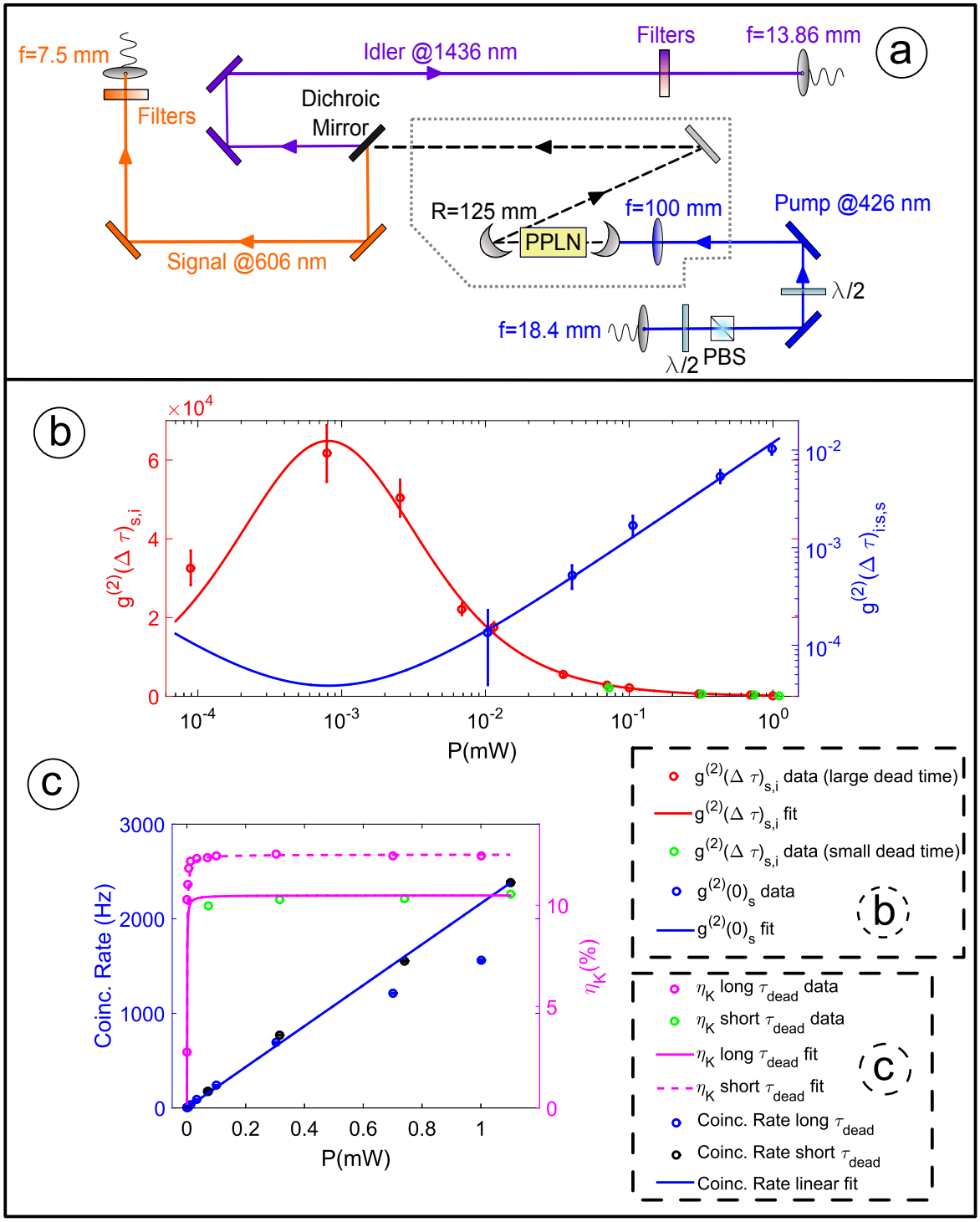

Figure 3. (a) Scheme of the free space setup. The idea is to be very similar to the one that would be used with the cavity. **(b) Cross-correlation, heralded auto-correlation & (c) coincidences rates, Klyshko efficiency** The solid lines show fits to the measured data (circles). Details given in the text.

FSR of the signal and idler photons. We observe a comb-like structure below the exponential envelope due to multiple frequency modes.

The linewidth of the biphoton $\Delta\nu$ (FWHM) is defined from the correlation time τ_c as $\tau_c = \frac{ln2}{\pi\Delta\nu} = \frac{ln2}{2\pi\Delta\nu_i} + \frac{ln2}{2\pi\Delta\nu_s}$, where $\Delta\nu_i$ corresponds to the idler linewidth and $\Delta\nu_s$ to the signal linewidth. Analysing this through the sum of two exponential functions, values of the linewidth of $\Delta\nu_i$ =**1.87 MHz** for the idler and $\Delta\nu_s$ =**2.87 MHz** for the signal are reported corresponding to a correlation time of the photon-pair of **97.4 ns** and to a biphoton linewidth of **2.26 MHz**.

In the same figure we can see the frequency distribution of the coincidences obtained through the Fourier transform of the previous coincidence data (right inset picture). Using a Lorentzian fit it can be found a FSR of **261 MHz**. Finally, using these results, the finesse of the cavity is calculated giving a value of **140** for the idler and **91** for the signal.

In the same histogram we show the time window of 400 ns used to analyse the data and the coincidences. This value was chosen since above this point the coincidences inside the window start to saturate. In order to keep consistence the same value of 400 ns remains constant over all the data analysis.

- **Number of modes:** If the coincidences histogram of the previous experiment is zoomed in as can be better seen in the left inset graph of Fig. 4 (b) many peaks are distinguished (for this histogram the bin size corresponds to the resolution of the detection method: 0.32 ns). In the simulations already done in the supplemental material of [3] it is shown that the relation between the width of these peaks and their separation can provide the number of modes that are generated inside the cavity. For this reason, a fit to ten Lorentzian curves is done in order to extract an averaged width of these peaks and their separation matches the inverse of the FSR that we already know.

  Using again the simulation in the previous paper we find a ratio width-separation of 0.369 $\pm$ 0.004, which suggests that **3 modes** are generated inside the cavity. However, this number sets a lower bound due to a possible limitation by the jitter of the detector.

- **Coincidences experiment:** This experiment is analogous to the one already presented in the section 4 with the fourth mirror as the only difference in its scheme. The dependence of the $g^{(2)}_{s,i}(\Delta t)$ with the pump power can be seen in the Fig. 4 (c) where the same model as before was used. The main differences on these parameters come from the higher coherence time of the photons and from the escape efficiency (discussed below) of the resonator. Again, the explanation of the shape of the curve is the same as before but with smaller values of the $g^{(2)}_{s,i}(\Delta t)$. At its maximum, a cross-correlation value of 224 is reported. Also at higher pump powers the pairs of photons show correlations with values of 3.5 for the 1 mW case.

  On the other hand, a coincidence rate depending linearly on the pump power with a slope of 333 $\frac{counts}{s \cdot mW}$ is also reported as can be seen in the Fig. 4 (d) *left axis*.

- **Escape efficiency:** In order to calculate the escape efficiency of the cavity, firstly, it is necessary to look at the Klyshko efficiency in the Fig. 4 (d) *rigth axis*. Here we observe an effect different from the one seen in the free space experiment since the efficiency at increasing powers continues growing after a flat regime. One possible explanation of this could be that the power is already high enough to generate multiple pairs which would artificially increase the Klyshko efficiency due to a higher number of signal counts.
  If we only look at the points that are not in this multi pair generation regime, values of the Klyshko efficiency for both, idler and signal are obtained: $\eta_K^I = 1.21\%$ and $\eta_K^S = 2.75\%$. From here, using the detection efficiency of the detectors, heralding efficiencies are calculated: $\eta_H^I = 12.1\%$ and $\eta_H^S = 4.58\%$.
  Finally, if we correct by the transmission efficiency between the detectors and the output of the cavity ($\eta^I = (30 \pm 10)\%$ and $\eta^S = (34.1 \pm 0.7\%)$ we find the escape efficiency: $\eta_{SC}^I = (40 \pm 13)\%$ and $\eta_{SC}^S = (13.4 \pm 0.3)\%$.
- **Cavity lock:** In order to have signal photons resonant with the quantum memory transition, the cavity has to be stabilised to the reference beam.
  With the error signal generated trough the PD2 and the Pound Drever Hall protocol [12] it is possible to keep the cavity locked and stable. We tested this scheme and its stability in trials of more than 3 hours.
  One drawback of using the reference beam to lock the resonator is that it follows the same optical path as the generated single photons. In order to avoid its arrival to the detectors, a chopper wheel was installed (see Fig. 4 (a)). The mechanical design of this wheel is optimized in order to allow the alternative pass of the reference beam and the generated photons, hence when the single photons are detected the reference beam is blocked and vice versa.
  One more chopper wheel synchronised with the already existing one should be installed in front of the telecom fibre in order to make possible single photon measurements with the cavity locked.

6. Conclusions

In this work, we have designed, built and characterised successfully a new photon pair source compatible with solid state QM. In a first step, the source was operated in free space configuration. Normalized $g_{s,i}^{(2)}(\Delta t)$ values up to $6 \cdot 10^4$ were measured and a single photon generation with $g_{i:s,s}^{(2)}(\Delta t)$ as low as $1.3 \cdot 10^{-4}$ was demonstrated. In a second step, with the crystal already embedded in the resonator, a $g_{s,i}^{(2)}(\Delta t)$ value around 224 was also shown.

Although the finesse is not as high as the one of the previous cavity, narrower photons have been reported, fulfilling the main goal of this thesis. The reason of having smaller finesse is thought to be caused by a more lossy crystal, a fact that is also consistent with the lower escape efficiency observed. Its exchange is an option for a

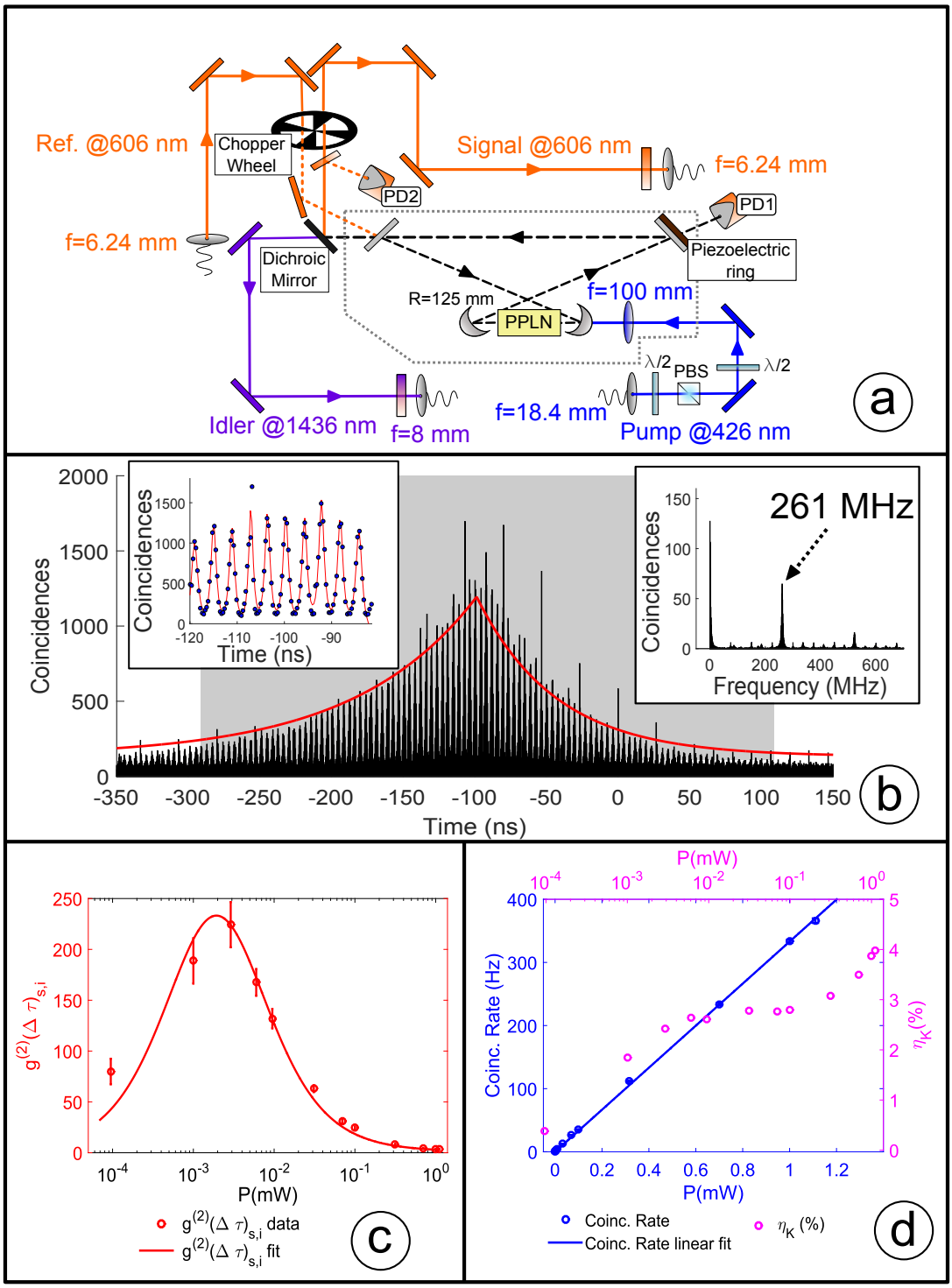

Figure 4. Scheme of the cavity enhanced setup: The cavity is closed and a reference beam to lock the cavity is also implemented. **(b) Coincidence histogram:** The main figure shows a histogram for temporally resolved cross-correlation of signal and idler at a pump power of 1 mW. The grey shaded region indicates the integration window of 400 ns. The left inset figure corresponds to a zoom in the middle of the coincidences histogram. The right inset figure is calculated through the Fourier transform of the main graph and is used to calculate the FSR. **(c) Cross-correlation & (d) coincidences rates, Klyshko efficiency.** The solid lines show fits to the measured data (circles). Details given in the text.

future improvement.

The next steps should include the installation of a filter cavity to keep only one mode of the three that are being reported in this text and the synchronisation of a second chopper wheel in the telecom path in order to make possible measurements with the cavity resonant to the reference beam. Also for the single photon storage the heralding efficiency must be improved.

In summary, the photons generated by this source represent a step forward in the improvement on the spin wave storage in Pr^{3+}:Y_2SiO_5 solid state QM. In addition, with the two sources and the already existing two Pr^{3+}:Y_2SiO_5 QM in the group the realisation of *heralded remote QM entanglement* will become possible.

Acknowledgments

I am deeply grateful to Andreas for teaching me almost all I know from this thesis, but also for all those funny moments and sharing his experience with me; to Hugues, for giving me this amazing opportunity and, of course, I would also like to give my biggest *THANK YOU* to the whole QPSA group for making me feel like *one more* since the first day and provide me the best educational experience in my life.

References

[1] Simon C, De Riedmatten H, Afzelius M, Sangouard N, Zbinden H and Gisin N 2007 *Physical Review Letters* **98** 190503
[2] de Riedmatten H and Afzelius M 2015 Quantum light storage in solid state atomic ensembles *Engineering the Atom-Photon Interaction* (Springer) pp 241–273
[3] Fekete J, Rieländer D, Cristiani M and de Riedmatten H 2013 *Physical Review Letters* **110** 220502
[4] Rieländer D, Lenhard A, Mazzera M and de Riedmatten H 2016 *arxiv* **1608.08943**
[5] Kwiat P G, Mattle K, Weinfurter H, Zeilinger A, Sergienko A V and Shih Y 1995 *Physical Review Letters* **75** 4337
[6] Christ A and Silberhorn C 2012 *Physical Review A* **85** 023829
[7] Wolfgramm F, de Icaza Astiz Y A, Beduini F A, Cerè A and Mitchell M W 2011 *Physical Review Letters* **106** 053602
[8] Krapick S, Herrmann H, Quiring V, Brecht B, Suche H and Silberhorn C 2013 *New Journal of Physics* **15** 033010
[9] Boyd G and Kleinman D 1968 *Journal of Applied Physics* **39** 3597–3639
[10] Kogelnik H and Li T 1966 *Applied Optics* **5** 1550–1567
[11] Sekatski P, Sangouard N, Bussières F, Clausen C, Gisin N and Zbinden H 2012 *Journal of Physics B: Atomic, Molecular and Optical Physics* **45** 124016
[12] Drever R, Hall J L, Kowalski F, Hough J, Ford G, Munley A and Ward H 1983 *Applied Physics B* **31** 97–105